Journal of Applied Phycology
https://doi.org/10.1007/s10811-021-02619-5

High CO_2 increases lipid and polyunsaturated fatty acid productivity of the marine diatom *Skeletonema costatum* in a two-stage model

Min Wu[1,2] · Guang Gao[1] · Youwen Jian[1] · Juntian Xu[2,3,4]

Received: 2 August 2021 / Revised: 24 September 2021 / Accepted: 24 September 2021

Abstract

Lipid and polyunsaturated fatty acids (PUFA) from microalgae can be used as biodiesel and health care products. How to enhance their productivity is crucial for successful commercial production. In this study, a two-stage model was used to stimulate the production of lipids and PUFA in a bloom-forming marine diatom *Skeletonema costatum*. Cells were cultured in ambient air (0.04% CO_2) in the first stage and transferred to two high CO_2 levels (5% and 10%) in the second stage. The medium CO_2 level (5%) increased both specific growth rate and lipid content and hence almost doubled lipid productivity compared to 0.04% CO_2 level. Although a 10% CO_2 level induced the highest lipid content, it had negative effects on the specific growth rate and soluble carbohydrate synthesis, and the lipid productivity was not as high as 5% CO_2. Neither CO_2 level affected the cell size, chlorophyll *a* content, or soluble protein content. High CO_2 levels also increased the synthesis of PUFA, e.g., eicosapentaenoic acid (EPA) and docosahexaenoic acid (DHA). Although high CO_2 levels increased iodine value and decreased the cetane number of oil exacted from *S. costatum*, they fall in the range of the European standard, suggesting its suitability for biodiesels. These findings indicate that a two-stage model with high CO_2 induction is an effective approach for the production of biodiesel and PUFA from *S. costatum*, which could be used in both biofuel and health care markets.

Keywords Algae · Biochemical composition · Biofuel · CO_2 · Fatty acids · Lipid

Introduction

Increasing CO_2 due mainly to anthropogenic activities is causing a series of environmental problems, including global warming, ocean acidification, marine heatwaves, etc. These climate change and extreme weather events are leading to severe ecological risks and social problems, such as biodiversity loss, species extinction, harmful algal blooms, food security, and even human mortality (IPCC 2018). To reduce carbon emission, the use of carbon-zero bioenergy to replace fossil fuels is deemed as a feasible and effective approach (Reid et al. 2020).

Biofuels have developed to the 3rd generation that identifies the viability of microalgae due to their high yield of biofuel and easy extraction apart from without competing for arable land with crops (Subhadra and Edwards 2010; Gao et al. 2019a). A variety of microalgae, including freshwater and seawater species, have been examined for biofuel production suitability and even some macroalgae have been considered (Adeniyi et al. 2018; Gao et al. 2020). After reviewing previous studies, we found that chlorophyte microalgae, such as *Chlorella* and *Dunaliella*, and the eustigmatophyte *Nannochloropsis*, have received much more attention thanks to their advantages in growth rates and lipid content (Dickinson et al. 2017; Peng et al. 2020). Diatoms, in spite of their rich diversity and high contribution to marine primary production, receive little attention in the field of biofuel though recent studies show the potential and advantages of diatoms in bioenergy

Min Wu and Guang Gao contributed equally to this work.

✉ Guang Gao
guang.gao@xmu.edu.cn

1 State Key Laboratory of Marine Environmental Science & College of Ocean and Earth Sciences, Xiamen University, Xiamen 361005, China

2 Jiangsu Key Laboratory of Marine Biotechnology, Jiangsu Ocean University, Lianyungang 222005, China

3 Jiangsu Key Laboratory of Marine Bioresources and Environment, Jiangsu Ocean University, Lianyungang 222005, China

4 Co-Innovation Center of Jiangsu Marine Bio-Industry Technology, Jiangsu Ocean University, Lianyungang 222005, China

Published online: 11 October 2021

sources (Levitan et al. 2014; Gao et al. 2019a). In addition to biofuel, lipids from microalgae could be an ideal source to supply polyunsaturated fatty acids (PUFA) that are broadly known for their beneficial effects on human health (Jiang et al. 2016; Saini and Keum 2018). Humans must ingest DHA and EPA from food since they cannot synthetize these long-chain PUFA in vivo. The majority of supplements of DHA and EPA are from marine fish oil until now, while the rising demand has led to overfishing (Boelen et al. 2013). Therefore, increasing attention is played to microalgae that have high PUFA contents and rapid growth rates apart from their environmental favorability.

Enhancing lipid content is essential for obtaining high lipid productivity. Microalgae usually increase the synthesis of lipids under stressful environments (Jaiswal et al. 2020). For instance, nitrogen or silicon deficiency has been proven to be an efficient technique to induce lipid accumulation in diatoms (Brennan and Owende 2010; Jiang et al. 2016; Gao et al. 2019a). The disadvantage of stress stimulus is that it can commonly reduce growth rates in spite of its stimulation in lipid synthesis (Jiang et al. 2016). To balance the growth rates and lipid content is a challenge for lipid production. Accordingly, a two-stage culture model is proposed to address this challenge, in which algae are cultured in favorable conditions in the first stage to maintain high growth rates and suffer from environmental stress, including nutrient, temperature, salinity, metal ions, irradiance, to induce lipid accumulation in the second stage (Su et al. 2011; Sibi et al. 2016; Gao et al. 2019a). The culture period for the second stage is usually very short to reduce its negative effects on growth. Therefore, a two-stage model has higher lipid productivity compared to the regular one-stage culture method (Su et al. 2011; Gao et al. 2019a). The two-stage culture model has been successfully used for *Nannochloropsis oculata* (Aléman-Nava et al. 2017) and *Chlorella* sp. (Nayak et al. 2019). Our recent study also applied this model to *Skeletonema costatum* with co-limitation of nitrogen and silicon used in the second stage (Gao et al. 2019a). However, little is known whether high CO_2 levels would induce more lipid accumulation in *S. costatum*.

Skeletonema costatum is a bloom-forming alga, with high growth rates when nutrients are abundant (Gao et al. 2018a). Furthermore, it has high tolerance against harsh culture conditions, suggesting an ideal biofuel source according to the strain selection criteria (Dickinson et al. 2017). Here, we proposed that the two-stage model with high CO_2 treatment in the second stage would enhance the productivity of lipid and PUFA in *S. costatum*. In this study, we test the hypothesis via growing *S. costatum* in a two-stage model and assessing its growth rates, lipid content, and fatty acid profile.

Materials and methods

Species collection

Skeletonema costatum was originally isolated from coastal waters of the Yellow Sea (34°42′36.55″N, 119°29′24.37″E), China. Before the experiment, cells of *S. cotatum* were cultured with natural seawater enriched with F/2 medium at 20 °C in an incubator (GXZ-500B, Ningbo, China) for 7 days, and the light density was 200 μmol photons m^{-2} s^{-1} with a 12-h:12-h light–dark cycle. Then the cells in the exponential growth phase were collected for the following experiment.

Experimental design

A two-stage culture model was designed in this study. The cells were first cultured in a semi-continuous mode for 5 days and a stable growth rate (~0.92 day^{-1}) was obtained (the first stage). The culture was aerated with the ambient air (0.04% CO_2) that was filtered through a 0.22-μm filter (Millipore, USA) during this stage. Then partial cells were transferred to 5% and 10% CO_2 conditions for 6 h induction (the second stage). The period of 6 h was chosen because longer periods of stress induction would lead to significant decreases in growth, which hinder the enhancement of lipid productivity (Gao et al. 2019a). The enriched CO_2 was supplied by a CO_2 enricher (CE100C-2, Ruihua, China) that could output CO_2 levels with a variation less than 3% of setting values. The cells kept in ambient air were set as control, termed one-stage model. The initial cell density for each CO_2 condition was 1×10^6 cells mL^{-1}, and there were three replications under each CO_2 condition. All physiological and biochemical parameters in the following sections were measured after 6 h induction.

Measurement of growth and cell size

Cell density was measured by a spectrophotometric method. Two milliliters of algal suspensions from each CO_2 condition were scanned with a microplate reader (Thermo, Multiskan GO, USA), and the OD value at 680 nm was recorded. The cell density was determined with the OD value and a standard curve (Gao et al. 2019a). The cell size was measured with a graticule under a microscope (DM500, Leica, Germany).

Measurement of photosynthetic pigments

The contents of chlorophyll *a* (Chl *a*) and carotenoid were determined according to Gao et al. (2009). Specifically,

50 mL of algal suspensions were filtered onto a GF/F membrane (25 mm, Whatman, UK) and then extracted by 5 mL of methanol overnight at 4 °C under darkness. After centrifugation (5000 × *g*, 10 min), the supernatant was scanned by a microplate reader (Thermo, Multiskan GO, USA). The optical density values at 480 nm, 510 nm, 632 nm, 665 nm, and 750 nm were used to calculate the concentrations of Chl *a* and carotenoid according to the following equations:

$$Chla(\mu gmL^{-1}) = 13.2654 \times (A665 - A750) - 2.6839 \times (A632 - A750);$$

$$Carotenoid(\mu gmL^{-1}) = 7.6 \times ((A480 - A750) - 1.49 \times (A510 - A750));$$

The contents (pg cell^{-1}) of Chl *a* and carotenoid were determined by cell density and pigment concentration (μg mL^{-1}).

Measurement of biochemical composition

The soluble protein content of the algae was determined by the modified Bradford method (Bradford 1976). Algal cells were collected via centrifuging (5000 × *g*, 10 min) 5 mL of algal suspensions and broken via freezing–thawing three times. Then 5 mL of PBS buffer (0.143 mol L^{-1} NaH_2PO_4 and 0.013 mol L^{-1} Na_2HPO_4) was added, and the solution was shaken in an ultrasonic cleaner for 1 h before the centrifugation (5000 × *g*, 10 min). Four milliliter Coomassie Brilliant Blue solution (100 mg G-250, dissolved in 50 mL of 95% ethanol solution, mixed with 100 mL of 85% phosphoric acid, and added with water to 1000 mL) was added to 1 mL of the supernatant. After mixing, the mixture was kept at room temperature for 3 min before being measured at 595 nm with a microplate reader (Thermo, Multiskan GO, USA). The soluble protein concentration (μg mL^{-1}) of the algae was determined according to a protein standard curve. The soluble protein content (% DW) was calculated from the dilution factor, cell concentration, and dry weight (DW).

The soluble carbohydrate was determined by a modified anthrone-sulfuric acid colorimetric method (Deriaz 1961). Algal cells were collected by centrifuging (5000 × *g*, 10 min) 5 mL of algal suspensions and broken by freezing–thawing three times. Then 5 mL of PBS buffer (0.143 mol L^{-1} NaH_2PO_4 and 0.013 mol L^{-1} Na_2HPO_4) were added, and the solution was shaken in an ultrasonic cleaner for 1 h and boiled for another hour. After centrifugation (5000 × *g*, 10 min), 1 mL supernatant was added to 4 mL of sulfuric acid-anthrone (0.2 g anthrone dissolved in 100 mL of concentrated sulfuric acid). After boiling for 10 min, the mixture was rapidly cooled to room temperature, and the absorbance was measured at 620 nm with a microplate reader (Thermo, Multiskan GO, USA). The soluble carbohydrate concentration is determined according to a standard curve. The soluble carbohydrate content (% DW) was calculated from the dilution factor, cell concentration, and dry weight (DW).

The contents of lipids and fatty acids (FA) were measured according to Gao et al. (2019a). Lipid productivity is the production of lipid during 6 h culture. Quantification of FA was based on peak areas of individual peaks identified, expressed as a percentage of the total peak areas for total fatty acid methyl esters (FAME).

Properties of oil from *S. costatum*

Physical characteristics of oil exacted from *S. costatum* were assessed based on the number of double bonds, chain length, and proportion of each fatty ester component in total fatty acids. As important indexes for physical characteristics of diesel, iodine value (IV) and cetane number (CN) are used to assess the quality of biodiesel from *S. costatum* according to Gao et al. (2019a).

Statistical analysis

Results in this study were expressed as means of three replicates ± standard deviation. Data were analyzed with the software SPSS v.23. The data conformed to a normal distribution (Shapiro–Wilk, $P > 0.05$) and variances were equal (Levene's test, $P > 0.05$). One-way univariate analysis of variance (ANOVA) was conducted to analyze the effects of CO_2 on biomass density, cell diameter, Chl *a* content, carotenoid content, soluble protein content, soluble carbohydrate content, total lipid content, lipid productivity, iodine value, and cetane number. One-way multivariate ANOVA (MANOVA) was conducted to assess the effect of CO_2 on the composition of fatty acids. The least significant difference (LSD) was conducted for post hoc investigation. A confidence interval of 95% was set for all tests.

Results

The effects of CO_2 on the growth and cell size of *S. costatum* were first investigated (Fig. 1). CO_2 had a significant effect on biomass density (ANOVA, $F_{(2,6)} = 31.326$, $P = 0.001$). Post hoc LSD comparison ($P = 0.05$) showed that cells cultured at 5% CO_2 had the highest biomass density and 10% CO_2 reduced growth although the decrease was not statistically significant (Fig. 1A). Compared to control, 5% CO_2 enhanced biomass density by 52.60%. In contrast, CO_2 did not affect cell diameter (ANOVA, $F_{(2,6)} = 0.929$, $P = 0.445$) that showed a narrow range (5.00–5.12 μm) under different CO_2 conditions (Fig. 1B).

Photosynthetic pigments of *S. costatum* under different CO_2 levels were also measured (Fig. 2). CO_2 (ANOVA, $F_{(2,6)} = 0.100$, $P = 0.906$) did not affect Chl *a* content that ranged from 0.14 to 0.15 pg cell^{-1} under different conditions (Fig. 2A). Carotenoid content varied with CO_2 concentration

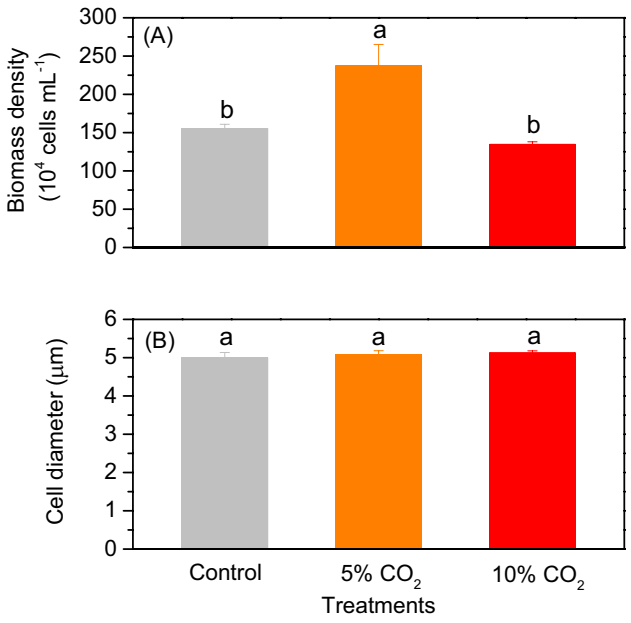

Fig. 1 Effects of CO_2 concentrations on biomass density (**A**) and cell diameter (**B**) of *S. costatum* after 6 h induction culture. The initial cell density was 1×10^6 cells mL^{-1}, and the air culture was set as the control, representing the one-stage culture model. Different lowercase letters represent significant differences among treatments (LSD, $P < 0.05$). The error bars indicate standard deviations ($n = 3$)

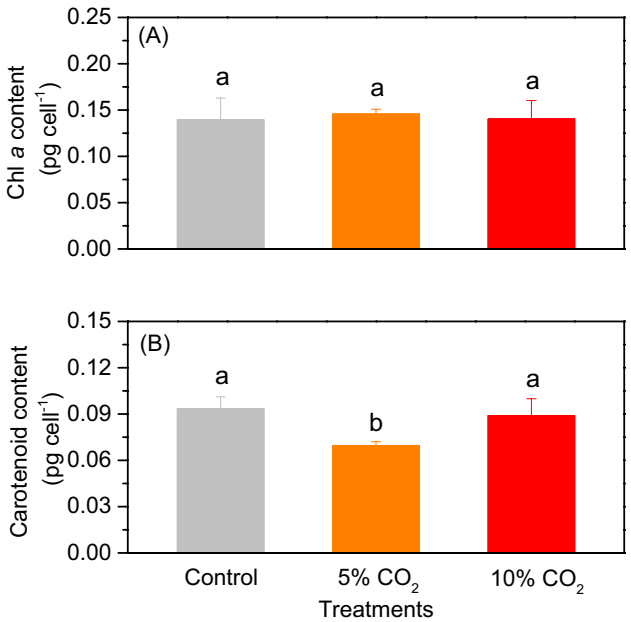

Fig. 2 Effects of CO_2 concentrations on the contents of Chl *a* (**A**) and carotenoid (**B**) of *S. costatum* after 6 h induction culture. The air culture was set as the control, representing the one-stage culture model. Different lowercase letters represent significant differences among treatments (LSD, $P < 0.05$). The error bars indicate standard deviations ($n = 3$)

(ANOVA, $F_{(2,6)} = 7.598$, $P = 0.023$) and the lowest value (0.07 pg $cell^{-1}$) occurred at 5% CO_2 level, with the difference between control and 10% CO_2 insignificant (Fig. 2B). Compared to control, the carotenoid content was reduced by 25.43% when cells were cultured at 5% CO_2.

The biochemical composition of *S. costatum* cultured at various CO_2 levels was also estimated (Fig. 3). Content of soluble protein ranged from 4.23 to 5.82% DW, although the change among CO_2 treatments was not statistically significant (ANOVA, $F_{(2,6)} = 2.863$, $P = 0.134$). In contrast, CO_2 significantly affected the content of soluble carbohydrate (ANOVA, $F_{(2,6)} = 21.187$, $P = 0.002$). Post hoc LSD comparison ($P = 0.05$) showed that 10% CO_2 reduced the content of soluble carbohydrate by 30.89% compared to control, while 5% CO_2 did not have a significant effect.

In terms of the content of total lipids (Fig. 4A), it increased with CO_2 level (ANOVA, $F_{(2,6)} = 140.799$, $P < 0.001$), from 12.18 under control to 20.71% DW at 5% CO_2 and then to 22.74% DW at 10% CO_2. CO_2 also affected lipid productivity (ANOVA, $F_{(2,6)} = 191.641$, $P < 0.001$, Fig. 4B). Different from lipid content, the highest value for lipid productivity (18.43 ± 0.19 mg L^{-1}) occurred at 5% CO_2, followed by that (15.71 ± 0.97 mg L^{-1}) at 10% CO_2, which were, respectively, 92.94% and 64.44% higher than that under control.

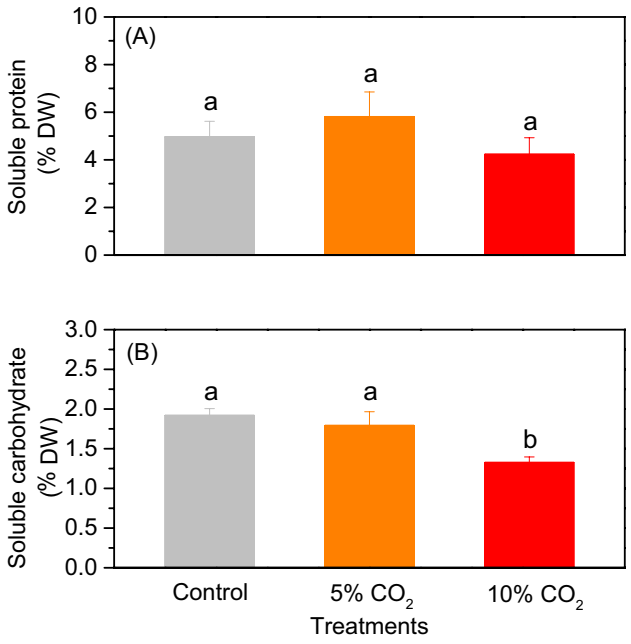

Fig. 3 Effects of CO_2 concentrations on the contents of soluble protein (**A**) and carbohydrate (**B**) of *S. costatum* after 6 h induction culture. The air culture was set as the control, representing the one-stage culture model. Different lowercase letters represent significant differences among treatments (LSD, $P < 0.05$). The error bars indicate standard deviations ($n = 3$)

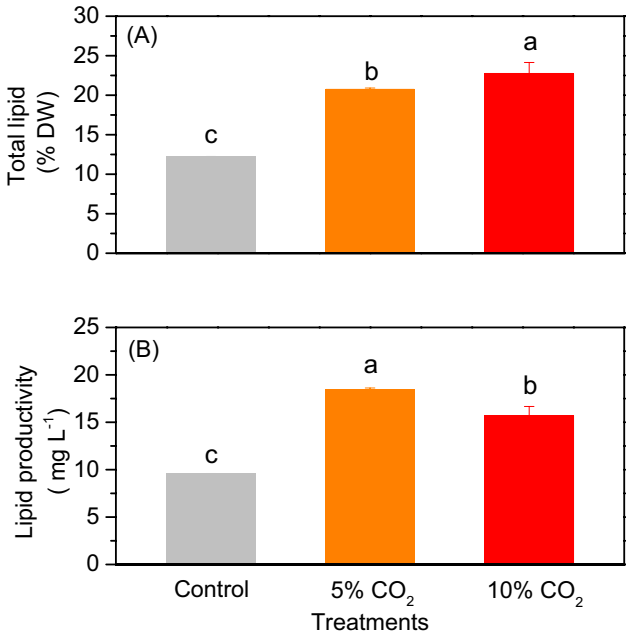

Fig. 4 Effects of CO_2 concentrations on total lipid content (**A**) and productivity (**B**) of *S. costatum* after 6 h induction culture. The air culture was set as the control, representing the one-stage culture model. Different lowercase letters represent significant differences among treatments (LSD, $P<0.05$). The error bars indicate standard deviations ($n=3$)

The fatty acid composition of *S. costatum* cultured under different CO_2 conditions was further investigated (Table 1). Among the identified 11 fatty acids, C16:0 is the dominant one, accounting for 33.82–41.98% of total FAME. C14:0 is the second most abundant fatty acid, followed by C16:1 and C18:0. C20:5(n-3) is the most abundant PUFA, having a proportion of 5.75–9.35% of total FAME. CO_2 did not affect the content of C12:0, C18:1(n-9c) or C18:2(n-6c) (Table 2). Compared to control, 5% CO_2 increased the contents of C14:0, C15:0, C16:1, C18:3(n-3), C20:5(n-3), C22:6(n-3), monounsaturated fatty acids (MUFA), and PUFA but reduced the contents of C16:0, C18:0, and saturated fatty acids (SFA); 10% CO_2 increased the contents of C15:0, C16:1, C20:5(n-3), C22:6(n-3), MUFA, and PUFA.

To assess the characteristics of lipid as biodiesel, iodine value and cetane number of lipid under different conditions were investigated (Fig. 5). Iodine value ranged 37.41–58.81 g I_2 100 g^{-1} oil and cetane number varied from 62.42 to 68.11. CO_2 affected both iodine value (ANOVA, $F_{(2,6)}=75.211$, $P<0.001$) and cetane number (ANOVA, $F_{(2,6)}=94.397$, $P<0.001$). Post hoc LSD comparison ($P=0.05$) showed that 5% CO_2 resulted in the highest iodine value, followed by 10% CO_2. On the other hand, 5% CO_2 led to the lowest cetane number and 10% CO_2 also reduced it compared to control.

Table 1 Effects of different CO_2 on fatty acid composition (% of total FAME) of *S. costatum* after 6 h induction culture. Values are means of three replicates ± standard deviation. The air culture was set as the control, representing the one-stage culture model. Significant differences ($P<0.05$) among the treatments are indicated by different lowercase letters ($n=3$). *SFA*, saturated fatty acids; *MUFA*, monounsaturated fatty acids; *PUFA*, polyunsaturated fatty acids

Fatty acid	Control	5% CO_2	10% CO_2
C12:0	0.11 ± 0.01^{a}	0.10 ± 0.01^{a}	0.10 ± 0.01^{a}
C14:0	18.24 ± 1.19^{b}	25.41 ± 0.12^{a}	18.54 ± 0.70^{b}
C15:0	0.90 ± 0.05^{c}	1.18 ± 0.01^{a}	1.04 ± 0.04^{b}
C16:0	41.98 ± 1.45^{a}	33.82 ± 0.27^{b}	41.50 ± 0.45^{a}
C16:1	9.56 ± 0.52^{b}	12.03 ± 0.2^{a}	11.71 ± 0.18^{a}
C18:0	8.53 ± 1.49^{a}	4.30 ± 0.29^{b}	8.51 ± 0.64^{a}
C18:1(n-9c)	0.27 ± 0.31^{a}	0.16 ± 0.01^{a}	0.34 ± 0.31^{a}
C18:2(n-6c)	0.36 ± 0.35^{a}	0.21 ± 0.01^{a}	0.45 ± 0.35^{a}
C18:3(n-3)	0.10 ± 0.02^{b}	0.21 ± 0.01^{a}	0.16 ± 0.06^{ab}
C20:5(n-3)	5.75 ± 0.32^{c}	9.35 ± 0.28^{a}	6.80 ± 0.04^{b}
C22:6(n-3)	0.93 ± 0.06^{c}	1.97 ± 0.09^{a}	1.62 ± 0.13^{b}
Unknown fatty acids	13.30 ± 0.14^{a}	11.25 ± 0.06^{b}	9.22 ± 0.29^{c}
SFA	69.75 ± 1.71^{a}	64.81 ± 0.50^{b}	69.7 ± 0.56^{a}
MUFA	9.82 ± 0.83^{b}	12.19 ± 0.19^{a}	12.04 ± 0.25^{a}
PUFA	7.13 ± 0.75^{c}	11.75 ± 0.35^{a}	9.04 ± 0.53^{b}

Discussion

Seawater is CO_2-limited for diatoms because CO_2 levels are around 10 µmol L^{-1} (20 °C) that is lower than half the saturation constant of ribulose-1,5-bisphosphate carboxylase/oxygenase (Rubisco) for most marine diatoms (Hopkinson et al. 2011). Therefore, the modest increase of CO_2 could commonly enhance algal photosynthesis and growth (Singh and Singh 2014; Hu et al. 2018; Lei et al. 2020). In this study, 5% CO_2 also increased the growth of *S. costatum* compared to the ambient air. This finding combined with our previous study (Gao et al. 2019b) indicates that *S. costatum* would benefit from rising CO_2, which is favorable for biofuel production from this species in future scenarios. However, further increases in CO_2 levels led to the decrease of growth in *S. costatum*. In addition to the positive effect of CO_2 enrichment, increased CO_2 can lead to the decrease of seawater pH, which can disturb the acid–base balance between extracellular and intracellular environments and thus impose negative effects on algal growth (Gao et al. 2018c). Increased CO_2 levels did not affect the cell size of *S. costatum* in the present study, and this finding is consistent with the result of *Phaeodactylum tricornutum* cultured at 1000 ppm CO_2 for 20 generations (Li et al. 2017). However, 1000 ppm CO_2 increased the cell volume of the coccolithophore *Gephyrocapsa oceanica* after 10 generations of acclimation. Therefore, the response of cell size to increased CO_2 may be species-dependent.

Table 2 Multivariate analysis of variance of the effects of CO_2 on the fatty acid content of *S. costatum* after 6 h induction. DF means degree of freedom, F means the value of F statistic, and Sig. means *p*-value

Source	Fatty acid	DF	*F*	Sig
CO_2	C12:0	2	1.032	0.412
	C14:0	2	77.23	< 0.001
	C15:0	2	49.264	< 0.001
	C16:0	2	79.665	< 0.001
	C16:1	2	48.02	< 0.001
	C18:0	2	19.748	0.002
	C18:1(n-9c)	2	0.354	0.716
	C18:2(n-6c)	2	0.517	0.621
	C18:3(n-3)	2	6.648	0.030
	C20:5(n-3)	2	168.95	< 0.001
	C22:6(n-3)	2	91.756	< 0.001
	Unknown fatty acids	2	354.103	< 0.001
	SFA	2	20.854	0.002
	MUFA	2	20.343	0.002
	PUFA	2	49.687	< 0.001
Error	C12:0	6		
	C14:0	6		
	C15:0	6		
	C16:0	6		
	C16:1	6		
	C18:0	6		
	C18:1(n-9c)	6		
	C18:2(n-6c)	6		
	C18:3(n-3)	6		
	C20:5(n-3)	6		
	C22:6(n-3)	6		
	Unknown fatty acids	6		
	SFA	6		
	MUFA	6		
	PUFA	6		

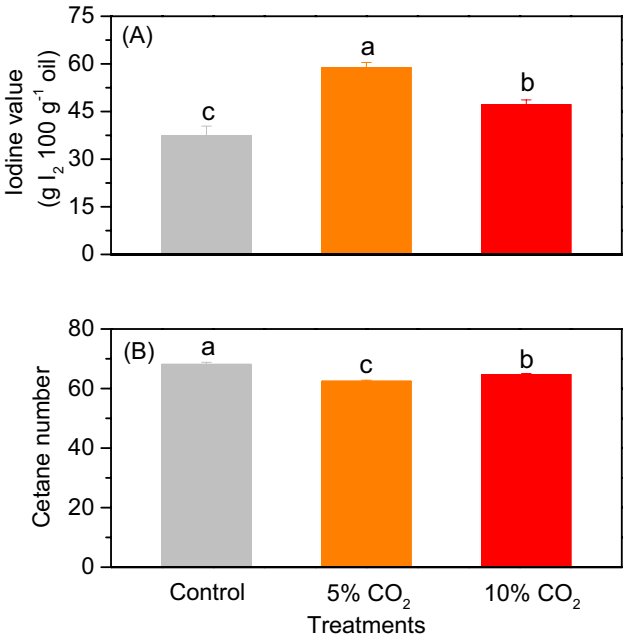

Fig. 5 Effects of CO_2 concentrations on iodine value (**A**) and cetane number (**B**) of biodiesels from *S. costatum* after 6 h induction culture. The air culture was set as the control, representing the one-stage culture model. Different lowercase letters represent significant differences among treatments (LSD, $P < 0.05$). The error bars indicate standard deviations ($n = 3$)

High CO_2 could usually reduce Chl *a* content because high CO_2 levels could enhance the sensitivity of algae to high light (Gao et al. 2016). Decreased light-capture pigments could avoid the overexcitation of electron transport and hence photoinhibition. However, high CO_2 did not affect Chl *a* content of *S. costatum* in this study, although 5% CO_2 did reduce carotenoid content. The different results from the previous studies may be due to the shorter exposure period used in this study. Increased CO_2 usually enhances carbohydrate content in algae because of the stimulating effects on photosynthesis (Mercado et al. 1999; Xu et al. 2017). Meanwhile, the mute effect of high CO_2 on carbohydrate content was also found in *Ulva rigida* and *Skeletonema marinoi* (Olofsson et al. 2015; Gao et al. 2017). In this study, 5% CO_2 did not affect carbohydrate content and 10% CO_2 even reduced it. High CO_2 may inhibit the photosynthetic carbon fixation of *S. costatum* through the decreased pH, which led to the decreased growth.

In contrary to carbohydrates, increased CO_2 induced lipid accumulation in *S. costatum*. Lipid biosynthesis requires carbon skeleton and ATP that could be supplied by photosynthesis. Therefore, increased CO_2 could stimulate lipid synthesis through increased photosynthetic rates. For instance, 0.2% CO_2 increased lipid content in *U. rigida* by 17–34% under different nitrate and temperature conditions compared to 0.07% CO_2 (Gao et al. 2017). High CO_2 (1%) increased total lipids in *Dunaliella viridis* from 1.83 to 2.06 pg $cell^{-1}$ under *n*-limited conditions (Gordillo et al. 1998). In this study, although 10% CO_2 had negative effects on carbohydrate synthesis and growth of *S. costatum*, it induced the highest lipid content. Therefore, the increased lipid synthesis may not come from photosynthesis but from carbon and energy diversion from protein and carbohydrate, because the contents of protein and carbohydrate were reduced at the highest CO_2 level. Compared to protein and carbohydrates, the lipid is preferentially synthesized in stressful environments because it is cost-optimal for rebuilding cells after the stress (Rodolfi et al. 2009; Gao et al. 2018b).

Lipid productivity is a critical index for biodiesel production (Griffiths and Harrison 2009; Gao et al. 2019a) as it integrates two key desirable characteristics: growth rate and lipid content. In this study, two higher CO_2 levels

resulted in enhanced lipid productivity, particularly for 5% CO_2 that almost doubled lipid productivity compared to control. Although 10% CO_2 led to the decrease of algal growth, the lipid productivity was still higher compared to control due to higher lipid content. The highest lipid productivity (18.43 ± 0.19 mg L^{-1}) of *S. costatum* induced by 5% CO_2 in this study is lower than that (41.76–64.71 mg L^{-1} day^{-1}) in *Nannochloropsis* sp. but higher than that (9–13 mg L^{-1} day^{-1}) in some *Chlorella* strains (Gu et al. 2012; Zheng et al. 2021). It is worth noting that the lipid productivity in this study is based on 6 h rather than 24 h used by previous studies. Therefore, the lipid productivity would be further enhanced if the culture period is considered.

Higher CO_2 level (5%) increased MUFA and PUFA but reduced SFA in *S. costatum*. A similar trend was also found in *Scenedesmus obliquus* and *Chlorella pyrenoidosa* (Tang et al. 2011). The possible reason for this phenomenon is that higher CO_2 concentrations could stimulate enzymatic desaturation and hence increase the content of unsaturated fatty acids but reduce saturated fatty acids (Vargas et al. 1998; Tang et al. 2011). The finding in this study combined with previous studies indicates that high CO_2 cultured microalgae are favorable for supplying PUFA for humans. In terms of biodiesel quality, lower iodine values and higher cetane numbers are desirable for biodiesels (Francisco et al. 2010; Gao et al. 2019a). The European standard (EN 14,214) defines a maximum of 120 g I_2 $(100\ g)^{-1}$ oil for iodine value and a minimum of 51 for cetane number. In the present study, the increased synthesis of unsaturated fatty acids in *S. costatum* cultured under higher CO_2 levels led to the higher iodine value and lower cetane number. However, even the highest iodine value and the lowest cetane number conform to the European standard, indicating that oil exacted from *S. costatum* cultured at higher CO_2 levels is still suitable to be used as biodiesels.

Conclusions

This study investigated the effects of high CO_2 levels on the production of lipid and fatty acids of a bloom-forming diatom in a two-stage model for the first time. The medium CO_2 level (5%) is proved to be optimal for lipid and PUFA production as it enhanced both the specific growth rate and lipid content. Further increase in CO_2 level had negative effects on the specific growth rate of *S. costatum* and then reduced the lipid productivity compared to 5% CO_2. The lipid from *S. costatum* cultured at higher CO_2 levels is favorable for PUFA production and also suitable for biodiesel.

Acknowledgements This work was supported by the National Key Research and Development Program of China (2018YFD0900703), the National Natural Science Foundation of China (42076154), the Fundamental Research Funds for the Central Universities (20720200111), and the MEL Internal Research Program (MELRI2004).

Data availability The raw data in the present study are available from the corresponding author on reasonable request.

Declarations

Conflict of interest The authors declare no competing interests.

References

Adeniyi OM, Azimov U, Burluka A (2018) Algae biofuel: current status and future applications. Renew Sustain Energy Rev 90:316–335

Aléman-Nava GS, Muylaert K, Bermudez SPC, Depraetere O, Rittmann B, Parra-Saldivar R, Vandamme D (2017) Two-stage cultivation of *Nannochloropsis oculata* for lipid production using reversible alkaline flocculation. Bioresour Technol 226:18–23

Boelen P, van Dijk R, Damsté JSS, Rijpstra WIC, Buma AGJ (2013) On the potential application of polar and temperate marine microalgae for EPA and DHA production. AMB Express 3:26

Bradford MM (1976) A rapid and sensitive method for the quantitation of microgram quantities of protein utilizing the principle of protein-dye binding. Anal Biochem 72:248–254

Brennan L, Owende P (2010) Biofuels from microalgae-a review of technologies for production, processing, and extractions of biofuels and co-products. Renew Sustain Energy Rev 14:557–577

Deriaz R (1961) Routine analysis of carbohydrates and lignin in herbage. J Sci Food Ag 12:152–160

Dickinson S, Mientus M, Frey D, Amini-Hajibashi A, Ozturk S, Shaikh F, Sengupta D, El-Halwagi MM (2017) A review of biodiesel production from microalgae. Clean Technol Envir 19:637–668

Francisco EC, Neves DB, Jacob-Lopes E, Franco TT (2010) Microalgae as feedstock for biodiesel production: carbon dioxide sequestration, lipid production and biofuel quality. J Chem Technol Biot 85:395–403

Gao G, Gao KS, Giordano M (2009) Responses to solar UV radiation of the diatom *Skeletonema costatum*(Bacillariophyceae) grown at different Zn^{2+}concentrations. J Phycol 45:119–129

Gao G, Clare AS, Rose C, Caldwell GS (2017) Eutrophication and warming-driven green tides (*Ulva rigida*) are predicted to increase under future climate change scenarios. Mar Pollut Bull 114:439–447

Gao G, Beardall J, Bao M, Wang C, Ren WW, Xu JT (2018a) Ocean acidification and nutrient limitation synergistically reduce growth and photosynthetic performances of a green tide alga *Ulva linza*. Biogeosciences 15:3409–3420

Gao G, Clare AS, Chatzidimitriou E, Rose C, Caldwell G (2018b) Effects of ocean warming and acidification, combined with nutrient enrichment, on chemical composition and functional properties of *Ulva rigi*da. Food Chem 258:71–78

Gao G, Xia J, Yu J, Zeng XP (2018c) Physiological response of a red tide alga (*Skeletonema costatum*) to nitrate enrichment, with special reference to inorganic carbon acquisition. Mar Environ Res 133:15–23

Gao G, Wu M, Fu Q, Li XS, Xu JT (2019a) A two-stage model with nitrogen and silicon limitation enhances lipid productivity and biodiesel features of the marine bloom-forming diatom *Skeletonema costatum*. Bioresour Technol 289:121717

Gao G, Fu Q, Beardall J, Wu M, Xu J (2019b) Combination of ocean acidification and warming enhances the competitive advantage of *Skeletonema costatum* over a green tide alga *Ulva linza*. Harmful Algae 85:101698

Gao G, Liu W, Zhao X, Gao K (2021) Ultraviolet radiation stimulates activity of CO_2 concentrating mechanisms in a bloom-forming diatom under reduced CO_2 availability. Front Microbiol 12:590

Gao G, Liu Y, Li X, Feng ZH, Xu JT (2016) An ocean acidification acclimatised green tide alga is robust to changes of seawater carbon chemistry but vulnerable to light stress. PLoS One 11(12):e0169040

Gao G, Burgess JG, Wu M, Wang SJ, Gao KS (2020) Using macroalgae as biofuel: current opportunities and challenges. Bot Mar 63:355–370

Gordillo FJL, Goutx M, Figueroa FL, Niell FX (1998) Effects of light intensity, CO_2 and nitrogen supply on lipid class composition of *Dunaliella viridis*. J Appl Phycol 10:135–144

Griffiths MJ, Harrison ST (2009) Lipid productivity as a key characteristic for choosing algal species for biodiesel production. J Appl Phycol 21:493–507

Gu N, Lin Q, Li G, Tan YH, Huang LM, Lin JD (2012) Effect of salinity on growth, biochemical composition, and lipid productivity of *Nannochloropsis oculata* CS 179. Eng Life Sci 12:631–637

Hopkinson BM, Dupont CL, Allen AE, Morel FMM (2011) Efficiency of the CO_2-concentrating mechanism of diatoms. Proc Nat Acad Sci USA 108:3830–3837

Hu S, Wang Y, Wang Y, Zhao Y, Zhang XX, Zhang YS, Jiang M, Tang XX (2018) Effects of elevated pCO_2 on physiological performance of marine microalgae *Dunaliella salina* (Chlorophyta, Chlorophyceae. J Oceanol Limnol 36:317–328

Jaiswal KK, Banerjee I, Singh D, Sajwan P, Chhetri V (2020) Ecological stress stimulus to improve microalgae biofuel generation: a review. Octa J Biosci 8:48–54

Jiang X, Han Q, Gao X, Gao G (2016) Conditions optimising on the yield of biomass, total lipid, and valuable fatty acids in two strains of *Skeletonema menzelii*. Food Chem 194:723–732

Lei X, Jiang L, Zhang Y, Zhou GW, Lian JS, Lian JS (2020) Response of coralline algae *Porolithon onkodes* to elevated seawater temperature and reduced pH. Acta Oceanol Sin 39:132–137

Levitan O, Dinamarca J, Hochman G, Falkowski PG (2014) Diatoms: a fossil fuel of the future. Trends Biotechnol 32:117–124

Li FT, Beardall J, Collins S, Gao KS (2017) Decreased photosynthesis and growth with reduced respiration in the model diatom *Phaeodactylum tricornutum* grown under elevated CO_2 over 1800 generations. Global Change Biol 23:17–137

Mercado JM, Javier F, Gordillo L, Niell FX, Figueroa FL (1999) Effects of different levels of CO_2 on photosynthesis and cell components of the red alga *Porphyra leucosticta*. J Appl Phycol 11:455–461

Nayak M, Suh WI, Chang YK, Lee B (2019) Exploration of two-stage cultivation strategies using nitrogen starvation to maximize the lipid productivity in *Chlorella* sp. HS2. Bioresource Technol 276:110–118

Olofsson M, Lindehoff E, Frick B, Svensson F, Legrand C (2015) Baltic Sea microalgae transform cement flue gas into valuable biomass. Algal Res 11:227–233

Peng L, Fu D, Chu H, Wang ZZ, Qi HY (2020) Biofuel production from microalgae: a review. Environ Chem Lett 18:285–297

Reid WV, Ali MK, Field CB (2020) The future of bioenergy. Global Change Biol 26:274–286

Rodolfi L, Chini Zittelli G, Bassi N, Padovani G, Biondi N, Bonini G, Tredici MR (2009) Microalgae for oil: strain selection, induction of lipid synthesis and outdoor mass cultivation in a low-cost photobioreactor. Biotechnol Bioeng 102:100–112

Saini RK, Keum YS (2018) Omega-3 and omega-6 polyunsaturated fatty acids: dietary sources, metabolism, and significance-a review. Life Sci 203:255–267

Sibi G, Shetty V, Mokashi K (2016) Enhanced lipid productivity approaches in microalgae as an alternate for fossil fuels–a review. J Energy Inst 89:330–334

Singh SP, Singh P (2014) Effect of CO_2 concentration on algal growth: a review. Renew Sustain Energy Rev 38:172–179

Su CH, Chien LJ, Gomes J, Lin YS, Yu YK, Liou JS, Syu RJ (2011) Factors affecting lipid accumulation by *Nannochloropsis oculata* in a two-stage cultivation process. J Appl Phycol 23:903–908

Subhadra B, Edwards M (2010) An integrated renewable energy park approach for algal biofuel production in United States. Energy Policy 38:4897–4902

Tang D, Han W, Li P, Miao XL, Zhong JJ (2011) CO_2 biofixation and fatty acid composition of *Scenedesmus obliquus* and *Chlorella pyrenoidosa* in response to different CO_2 levels. Bioresour Technol 102:3071–3076

Vargas MA, Rodriguez H, Moreno J, Olivares H, Del Campo JA, Rivas J, Guerrero MG (1998) Biochemical composition and fatty acid content of filamentous nitrogen-fixing cyanobacteria. J Phycol 34:812–817

Xu Z, Gao G, Xu J, Wu HY (2017) Physiological response of a golden tide alga (*Sargassum muticum*) to the interaction of ocean acidification and phosphorus enrichment. Biogeosciences 14:671–681

Zheng S, Chen S, Zou S, Yan YW, Gao G, He ML, Wang CH, Chen H, Wang Q (2021) Bioremediation of *Pyropia*-processing wastewater coupled with lipid production using *Chlorella* sp. Bioresource Technol 321:124428